A fusion-intermediate state of HIV-1 gp41 targeted by broadly neutralizing antibodies

Gary Frey*[†], Hanqin Peng*, Sophia Rits-Volloch*[‡], Marco Morelli[§], Yifan Cheng[¶], and Bing Chen*[‖]

*Laboratory of Molecular Medicine, Children's Hospital, and Department of Pediatrics, Harvard Medical School, 320 Longwood Avenue, Boston, MA 02115; [†]Jack and Eileen Connors Structural Biology Laboratory, Harvard Medical School, 250 Longwood Avenue, Boston, MA 02115; [‡]Howard Hughes Medical Institute, 320 Longwood Avenue, Boston, MA 02115; [§]Program in Virology, Harvard Medical School, 250 Longwood Avenue, Boston, MA 02115; and [¶]Department of Biochemistry and Biophysics, University of California, San Francisco, CA 94158

Communicated by Stephen C. Harrison, Children's Hospital Boston, Boston, MA, January 10, 2008 (received for review December 18, 2007)

Most antibodies induced by HIV-1 are ineffective at preventing initiation or spread of infection because they are either nonneutralizing or narrowly isolate-specific. Rare, ''broadly neutralizing'' antibodies have been detected that recognize relatively conserved regions on the envelope glycoprotein. Using stringently characterized, homogeneous preparations of trimeric HIV-1 envelope protein in relevant conformations, we have analyzed the molecular mechanism of neutralization by two of these antibodies, 2F5 and 4E10. We find that their epitopes, in the membrane-proximal segment of the envelope protein ectodomain, are exposed only on a form designed to mimic an intermediate state during viral entry. These results help explain the rarity of 2F5- and 4E10-like antibody responses and suggest a strategy for eliciting them.

envelope glycoprotein | membrane fusion

HIV-1 infection generally induces a strong antibody response to the envelope glycoprotein [trimeric $(gp160)_3$, cleaved to $(gp120/gp41)_3$], the sole antigen on the virion surface. Most induced antibodies are ineffective in preventing infection, however, because they are either nonneutralizing or narrowly isolate-specific, and the virus replicates so rapidly that ongoing selection of neutralization resistant mutants allows viral evolution to "keep ahead" of high-affinity antibody production (1). Moreover, much of the antibody response may be to rearranged or dissociated forms of gp120 and gp41, on which the dominant epitopes may be either in hypervariable loops or in positions occluded on virion-borne envelope trimer. Rare, "broadly neutralizing" antibodies have been detected that recognize one of three relatively conserved regions on the envelope protein: the CD4-binding site (mAb b12) (2); carbohydrates on the outer gp120 surface (mAb 2G12) (3); and a segment of the gp41 ectodomain adjacent to the viral membrane (mAbs 2F5 and 4E10) (4, 5), often called the "membrane-proximal external region" (MPER). We seek to understand the molecular mechanisms of neutralization by these and other antibodies.

Fusion of viral and target-cell membranes initiates HIV-1 infection. Conformational changes in gp120 that accompany its binding to receptor (CD4) and coreceptor (e.g., CCR5 or CXCR4) lead to dissociation of gp120 from gp41 and a cascade of refolding events in the latter (6). In the course of these rearrangements, the N-terminal fusion peptide of gp41 translocates and inserts into the target-cell membrane. A proposed extended conformation of the gp41 ectodomain, with its fusion peptide thus inserted and the transmembrane anchor still in the viral membrane, has been called the "prehairpin intermediate" (7). It is the target of various fusion inhibitors, including T-20/enfuvirtide, the first approved fusion-inhibiting antiviral drug (8), and the characteristics of the intermediate have been deduced from the properties of these inhibitors or mimicries by short gp41 fragments (9). Subsequent rearrangements from the intermediate to the postfusion state of gp41 involve folding back of each of the three chains into a hairpin-like conformation, with two antiparallel α-helices connected by a disulfide-containing loop. This process brings the fusion peptide and transmembrane anchor, and hence the two membranes, close together at the same end of the refolded protein.

Where in this sequence of events do neutralizing antibodies intervene, and can any such antibodies neutralize more than a narrow range of isolates? The first step toward answering these questions is the preparation of biochemically homogeneous forms of the HIV envelope glycoprotein with defined and uniform antigenic properties, which include each of the principal states of the gp41 ectodomain: the prefusion, the prehairpin intermediate, and the postfusion conformations. We describe here stable, homogeneous preparations of trimeric HIV-1 envelope protein in relevant states. We show that the epitopes for the MPER antibodies, 2F5 and 4E10, are exposed only on the form of the envelope protein designed to mimic the prehairpin intermediate. These results help explain the rarity of 2F5- and 4E10-like antibody responses and suggest how one might design an immunogen to elicit them.

Results

Stable Conformations of HIV Envelope Glycoprotein. ***Gp140 trimer.*** Gp140, the ectodomain of the precursor gp160, is often produced to mimic the prefusion state of the envelope, based on structural studies of other viral fusion proteins, e.g., influenza hemagglutinin (10). The stability of HIV-1 gp140 varies greatly from strain to strain; it can be enhanced by adding a C-terminal trimerization tag such as the T4-fibritin "foldon" or the coiled-coil trimer derived from GCN4 (11, 12). Recombinant simian immunodeficiency virus (SIV) gp140 is a stable trimer even without such a tag (13). We have expressed gp140 proteins from a number of HIV-1 primary isolates, with and without trimer tags, to identify sequences that yield particularly stable gp140 trimers [supporting information (SI) Fig. 5]. A construct we call 92UG-gp140-Fd, derived from isolate 92UG037.8 and stabilized by a C-terminal foldon tag, has proved especially well behaved (Fig. 1). Its properties, analyzed by size-exclusion chromatography, sedimentation equilibrium, and chemical cross-linking, are shown in Fig. 2. Uncleaved gp140 from the same isolate but without the C-terminal foldon also yields stable trimer (data not shown), but the foldon form is easier to purify because of its higher affinity for Ni-nitrilotriacetic acid (NTA). To mimic even more closely the conformation of $(gp120/gp41)_3$ on the virion surface, we have made partially cleaved gp140 with human plasmin (see SI Fig. 6*I*).

Gp41-prehairpin intermediate. To produce biochemically homogeneous forms of additional conformations, we made two constructs designed to capture gp41 in the extended, prehairpin intermediate conformation. As shown in Fig. 1, gp41-inter has the following sequence: (HR2)-linker-[HR1-CC loop-HR2-MPER]-(trimerization tag), where HR1 and HR2 are the first and second "heptad

Author contributions: G.F. and B.C. designed research; G.F., H.P., S.R.-V., M.M., Y.C., and B.C. performed research; M.M. and Y.C. contributed new reagents/analytic tools; G.F. and B.C. analyzed data; and B.C. wrote the paper.

The authors declare no conflict of interest.

[‖]To whom correspondence should be addressed. E-mail: bchen@crystal.harvard.edu.

This article contains supporting information online at www.pnas.org/cgi/content/full/0800255105/DC1.

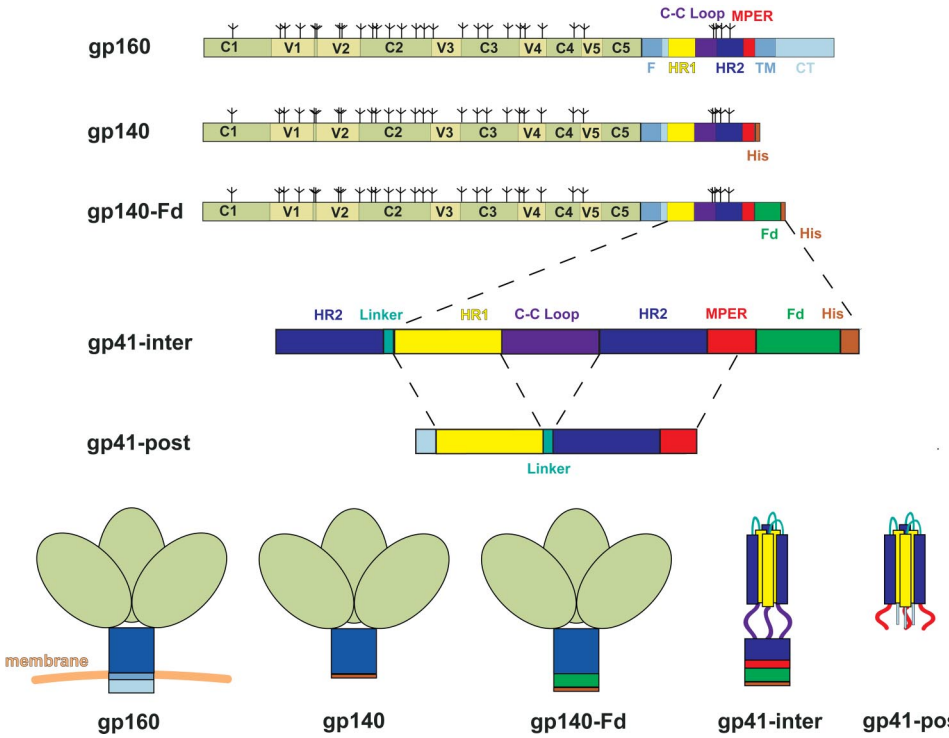

Fig. 1. Expression constructs. (*Upper*) Schematic representations of HIV-1 envelope glycoproteins; gp160, the full-length precursor. Various segments of gp120 and gp41 are designated as follows: C1–C5, conserved regions 1–5; V1–V5, variable regions 1–5; F, fusion peptide; HR1, heptad repeat 1; C–C loop, immunodominant loop with a conserved disulfide bond; HR2, heptad repeat 2; (see SI Fig. 9 for alignment); TM, transmembrane anchor; CT, cytoplasmic tail. Expression constructs are: gp140, uncleaved ectodomain of gp160 with a C-terminal His tag; gp140-Fd, uncleaved ectodomain of gp160 with a trimerization tag and a C-terminal His tag; gp41-inter, gp41 in the prehairpin intermediate conformation trapped by an N-terminal HR2 peptide and a C-terminal foldon tag; gp41-post, gp41 in the six-helix conformation with partial MPER. Glycans are represented by tree-like symbols. (*Lower*) Diagrams represent 3D organization of these protein species. Gp120 and gp41 in the prefusion state are shown in light green and light blue, respectively. The viral membrane is in orange. Other regions are colored as in the schematics above.

repeat" in gp41 (the segments that form helices in the postfusion trimer of hairpins) and the sequence in brackets is essentially the complete gp41 ectodomain, except for the fusion peptide. The "linker" is a short, flexible connector of serines and glycines. When gp41-inter chains trimerize, we expect the N-terminal HR2 segments to form a six-helix bundle with the HR1 segments; the C-terminal HR2 segments, constrained by the trimerization tag, will be unable to do so. The conformation of this construct can be pictured as the prehairpin intermediate captured by an HR2 peptide, such as T-20. We expressed gp41-inter by using sequences from two isolates: 92UG037.8 and HXB2, with foldon and trimeric GCN4, respectively. In both cases, the protein could be expressed in *Escherichia coli* and refolded *in vitro*. Controls showed that the N-terminal HR2 segment is required for refolding of bacterially expressed protein and for obtaining soluble, secreted protein from insect cells (data not shown). A similar construct with the gp41 sequence of SIVmac32H and the catalytic subunit of *E. coli* aspartate transcarbamoylase as trimer tag (14) could also be obtained as secreted protein from insect cells (data not shown), indicating that the overall design is robust and independent of the choice of a C-terminal trimerizing element.

Purified 92UG-gp41-inter is a monodisperse trimer (Fig. 2 *D* and E), stable after multiple rounds of gel-filtration chromatography. Its CD spectrum suggests a mixture of secondary structures (SI Fig. 7*A*). Negative-stain electron microscopy shows rod-like particles, 150 Å in length and ≈45 Å wide (Fig. 2*F*). The expected lengths for the N-terminal six-helix bundle and the C-terminal foldon are 75 and 28 Å, respectively. The intervening segment of ≈100 residues (C–C loop, HR2, and MPER) must have a relatively compact fold, to span just 45–50 Å of axial distance.

Gp41-postfusion six-helix bundle. Forms of postfusion gp41 that contain the complete MPER tend to aggregate. We have prepared a six-helix bundle construct that contains the full 2F5 epitope (LDKWANL) but lacks 4E10 epitope; we designate it "gp41-post" (Fig. 1). As refolded from *E. coli*-expressed inclusion bodies, gp41-post has all of the properties expected for a trimer of α-helical hairpins (SI Fig. 8).

Ligand Binding and Antigenic Properties of Envelope Protein in Distinct Conformational States. We have carried out binding experiments to verify the integrity of the 92UG-gp140-Fd trimer and to analyze its antigenic properties. The 92UG-gp140-Fd trimer binds CD4 with a K_d of 1.98 nM (Table 1 and SI Fig. 6*A*); the surface plasmon resonance (SPR) sensorgrams can be fit by a two-step binding model as used for binding of CD4 to gp120 core (15). Thus, the covalent linkage between gp120 and gp41 does not impede the conformational change in gp120 that accompanies CD4 binding. The 92UG-gp140-Fd trimer also binds mAb 2G12 (3) with high affinity (Table 1 and SI Fig. 6*B*), as expected, because the 92UG037 isolate is sensitive to neutralization by 2G12 (16). The trimer fails to bind the b12 IgG (2), consistent with the resistance of the isolate to neutralization by that mAb (16), but monomeric gp120 derived from 92UG037 does bind b12, with a K_d of 1.4 μM (ref. 15 and SI Fig. 6*C*). This affinity is ≈2 orders of magnitude weaker than measured for the same mAb with gp120 from isolates HXB2 or YU2 (17), probably because of a sequence difference in the CD4-binding loop [P369L, HXB2 numbering, a residue that makes direct contact with b12 (17)]. In addition, the 92UG-gp140-Fd trimer does not bind two other "nonneutralizing" CD4-binding site antibodies, b6 and 15e, despite high affinities of these two antibod-

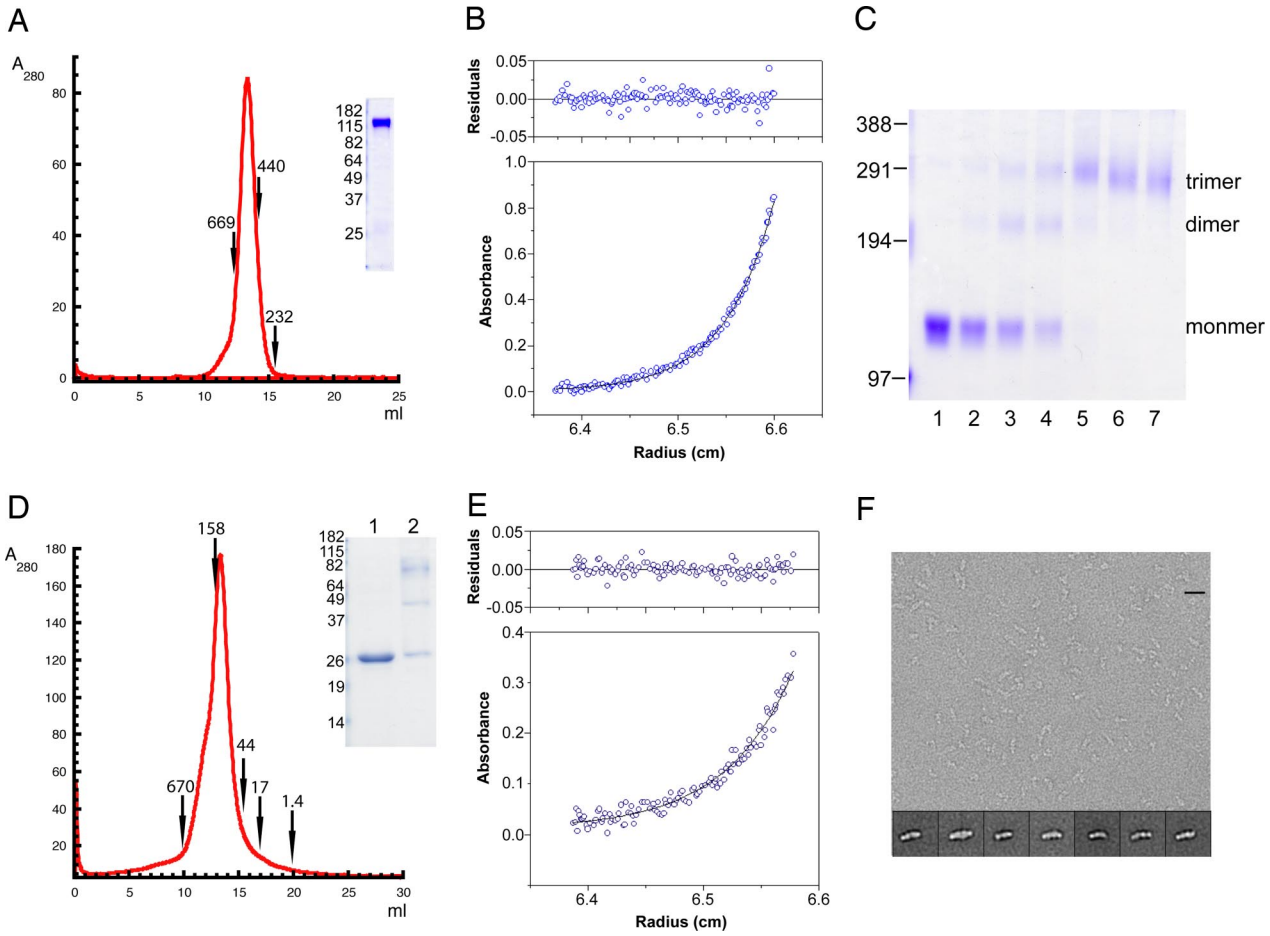

Fig. 2. Preparations of the prefusion and the prehairpin intermediate conformations of HIV-1 gp41. (*A*) Purified HIV-1 92UG-gp140-Fd trimer was resolved by gel-filtration chromatography on Superose 6. The apparent molecular mass was calculated by using as standards thyroglobulin (670 kDa), ferritin (440 kDa), and catalase (232 kDa). (*Inset*) Peak fractions were pooled and analyzed by Coomassie blue-stained SDS/PAGE. (*B*) Sedimentation equilibrium of 92UG-gp140-Fd trimer with a Beckman XL-A analytical ultracentrifuge at 4°C. Three protein concentrations (0.62, 1.24, 2.48 μM) and three rotor speeds (1,820, 3,567, and 5,897 $\times$ *g*) were used. The data shown were collected with the protein at 1.24 μM and rotor speed of 3,567 $\times$ *g*. Data were analyzed with a single-species model; partial specific volume was calculated as 0.686 ml/g, using the sugar content. The molecular mass is 409 $\pm$ 10 kDa. (*C*) 92UG-gp140-Fd trimer was treated with various concentrations (lanes 1–7, 0, 0.05, 0.25, 0.5, 1, 2, 5 mM) of ethylene glycol bis(succinimidylsuccinate). Cross-linked products were analyzed by SDS/PAGE in a 4% gel. The molecular mass standard was cross-linked phosphorylase *b* (Sigma). Dimeric and trimeric species of 92UG-gp140-Fd migrate faster than expected for their molecular mass, probably because of compactness after cross-linking. (*D*) 92UG-gp41-inter was expressed in *E. coli* and refolded *in vitro*. (*Inset*) The refolded protein was resolved by gel-filtration chromatography on Superdex 200. It migrates on SDS/PAGE at molecular mass ≈26 kDa when sample is boiled and reduced; when not boiled and not reduced, there is a ladder of three bands (≈26, 50, 80 kDa, respectively), corresponding to monomer, dimer, and trimer. (*E*) Sedimentation equilibrium of 92UG-gp41-inter with a Beckman XL-A analytical ultracentrifuge at 4°C. Three protein concentrations (0.98, 1.96, 3.92 μM) and three rotor speeds (16,380, 22,295, and 49,213 $\times$ *g*) were used. Data shown were collected with the protein at 3.92 μM and rotor speed of 22,295 $\times$ *g*. Data were analyzed with a single-species model; the molecular mass is 92 $\pm$ 6 kDa. (*F*) 92UG-gp41-inter examined by negative-stain electron microscopy. Raw image of a field (*Upper*) and selected images after class averaging to increase signal-to-noise (*Lower*). The dimensions of the rod-like molecules are ≈150 Å $\times$ 45 Å. (Scale bar: 20 nm.)

ies for 92UG-gp120 core (Table 1 and SI Fig. 6 *D* and *E*). We conclude that the position and orientation of gp120 in the prefusion trimer reduce accessibility of the CD4 site to antibodies, without impeding accessibility to CD4. Uncleaved 92UG-gp140-Fd also binds a CD4i (CD4-induced) mAb, 17b (18), but only in the presence of CD4, as expected (SI Fig. 6*F*). This result shows that the gp120 part of this trimer can undergo the conformational transition associated with formation of the bridging sheet, the docking site for mAb 17b (and for coreceptor), even when gp120 cannot fully dissociate, consistent with the similar observations from other groups (12).

Antibodies to gp41 include those in "cluster I," which bind the immunodominant, disulfide-containing loop between the two helical regions of the postfusion form, and those in "cluster II," which bind MPER epitopes. The 92UG-gp140-Fd trimer binds two cluster I mAbs, 240-D and 246-D (SI Fig. 6*G*), in accord with earlier observations that SIV gp140 trimer interacts with cluster I mAbs, KK41 and 9G3, and that cluster I epitopes are well exposed on HIV-1 virions (19–21). We note that mAb 9G3 has neutralizing activity (20). We also find strong binding of 240-D and 246-D with plasmin cleaved 92UG-gp140-Fd (data not shown), but because the cleavage is incomplete, we cannot make strong conclusions about the effects of gp120-gp41 cleavage on antibody affinity. Some previous reports suggest that cluster I and II epitopes are exposed on uncleaved, *oligomeric* gp140 but inaccessible on cleaved, disulfide-linked, *monomeric* SOS gp140 derived from the same strain (22). The conformational homogeneity of those preparations was not fully assessed, and the cluster I epitope in the SOS gp140 was also altered by the extra disulfide introduced.

The 92UG037 isolate is sensitive to neutralization by the broadly neutralizing, MPER-directed human monoclonal antibodies, 2F5 and 4E10 (16), and these two antibodies indeed recognize unfolded

Table 1. Binding rate constants derived from SPR analysis

Immobilized ligand	Flowing analyte	k_a, 1/ms		k_d, 1/s		K_d, M
		k_{a1}, 1/ms	k_{a2}, 1/s	k_{d1}, 1/s	k_{d2}, 1/s	1.98E-9
92UG-gp140-Fd	4DsCD4	2.39E5	2.11E-2	141E-2	7.38E-4	1.98E-9
92UG-gp140-Fd	2G12-Fab	5.35E4		9.58E-4		1.79E-8
b12 IgG	92UG-gp120	1.50E4		1.49E-2		9.93E-7*
b6 IgG	92UG-gp120	5.62E4		1.51E-4		2.69E-9*
15e IgG	92UG-gp120	4.85E4		3.18E-3		6.57E-8*
2F5 Fab	92UG-gp41-inter-Fd	1.00E4		1.39E-5†		1.38E-9
2F5 Fab	HXB2-gp41-inter-GCN4	6.82E3		6.11E-5†		8.96E-9
92UG-gp41-inter-Fd	2F5-Fab	1.53E5		4.96E-4		3.24E-9
2F5 Fab	T-20	4.54E5		2.17E-3		4.79E-9
2F5 Fab	2F5 epitope peptide‡	8.59E5		3.29E-3		3.83E-9
2F5 epitope peptide‡	2F5-Fab	2.82E5		1.50E-3		5.33E-9
92UG-gp41-inter-Fd	4e10 scFv	1.60E5		1.71E-4		1.07E-9*
His-4e10 scFv	HXB2-gp41-interf-GCN4	1.49E5		4.43E-4		2.98E-9*
4e10 epitope peptide§	4e10 scFv	3.69E4		6.85E-4		1.86E-8
2F5 Fab	92UG-gp41-post	1.66E3		2.43E-3		1.41E-6

*These binding constants were derived by fitting the sensorgram with a single concentration of analyte; results here for b12 IgG are essentially identical to those published previously by fitting runs with multiple concentrations (16).

†These sensorgrams are virtually flat during the dissociation phase, making accurate fitting very difficult. Thus, the actual off-rates are probably even slower than these listed here.

‡The short 2F5 epitope peptide used is ELLELDKWASL.

§The 4E10 epitope peptide is biotin-SLWNWFNITNWLWYIK.

92UG-gp140-Fd on a Western blot (Fig. 3*A*, *Inset*, lane 1, and Fig. 4*C*). The native trimer does not, however, bind mAb 2F5 under any of the conditions we tested by SPR. In particular, 92UG-gp140-Fd exhibits no interaction with a 2F5 surface, regardless of whether IgG or Fab was used for immobilization (Fig. 3*A*). We have also observed no binding of 2F5 IgG or Fab with immobilized gp140, at either 20° or 37°C. The presence or absence of the foldon tag has no effect, nor does partial plasmin cleavage (Fig. 3*A*). The 92-gp140-Fd trimer also fails to bind 4E10 Fab and shows only very weak binding to 4E10 IgG at high concentration (Fig. 4*A* and SI Fig. 6*H*). We conclude that the epitopes of 2F5 and 4E10 are either buried or in a nonantigenic configuration on the native gp140 trimer. This conclusion is consistent with published reports that mAb 2F5 does not bind the envelope protein on the surface of virions (23, 24). Other published experiments suggest a temperature-sensitive interaction with cell surface-expressed Env, but the structural heterogeneity of cleaved envelope protein on cell surfaces and the potential lipid-binding ability of 2F5 make those results difficult to interpret (25–27). The gp140 preparations reported to bind 2F5 all contain significant amounts of monomers, dimers, or aggregates (11, 22).

If mAbs 2F5 and 4E10 do not bind the ectodomain of the $(gp120/gp41)_3$ in the prefusion conformation found on virions, how do they neutralize? Several reports have provided evidence that 2F5 may target the fusion-intermediate conformation of gp41 (28, 29), but previous attempts to mimic the intermediate state have been limited largely to constructs containing only the HR1 and HR2 fragments (9), which could not be used to resolve the issue. In contrast, our gp41-inter constructs contain nearly the full-length gp41 ectodomain, including the full epitopes for 2F5 and 4E10. The data in Fig. 3*B* and SI Fig. 7*B* show that the Fab fragment derived from mAb 2F5 binds gp41-inter proteins very tightly (K_d <10 nM, with k_{off} <1.4 × 10^{-5} s^{-1}), regardless of the choice of isolate and trimerization tag (Table 1). (We used the Fab to avoid potential avidity effects with intact antibody). The estimated dissociation constant is relatively insensitive to which protein is immobilized on the chip. The complex of 2F5 Fab and 92UGgp41-inter protein can also be purified by gel-filtration chromatography (data not shown). The 4E10 single-chain Fv fragment (scFv) likewise bound strongly to gp41-inter proteins (K_d ≈1.1–2.9 nM; Fig. 4*B*, Table 1, and SI Fig. 7*D*). We used scFv because 4E10 Fab produced by papain digestion had weaker neutralizing activity than scFv and IgG, whereas the latter two were equally potent (M.M., M. Alam, B. Haynes, S. Harrison, and B.C., unpublished data). These observations suggest that 2F5 and 4E10 exert their neutralizing activity by binding an intermediate conformation of gp41. Kinetic studies of membrane fusion have shown that both 2F5 and 4E10, like T-20, are probably effective only in a small time interval during the fusion process (29, 30). Moreover, mutations in the gp41 core that destabilize the six-helix bundle enhance sensitivity of the mutant viruses to 2F5 neutralization (31).

Peptides that contain the 2F5 epitope, such as T-20, bind the 2F5 Fab, as expected (Fig. 3*D* and Table 1), but they dissociate much more rapidly than do the gp41-inter proteins (Table 1). Rapid dissociation has also been reported when the 2F5 epitope peptide is inserted into protein scaffolds other than gp41-inter (32). A peptide containing the full 4E10 epitope also bound more weakly to 4E10 scFv (K_d ≈18 nM) than did gp41-inter (Fig. 4*D* and Table 1). Thus, very strong binding by these two mAbs appears to be a specific consequence of incorporating the epitope into a prehairpin intermediate-like conformation.

As expected, postfusion gp41 binds the 2F5 Fab very weakly (K_d ≈1.4 μM; Table 1 and SI Fig. 8*D*), whereas a short epitope peptide ending with the same residue as gp41-post binds tightly (K_d ≈3.8–5.3 nM; Table 1). Thus, the 2F5 epitope in gp41-post does not have an optimal binding conformation, consistent with observations that the formation of the six-helix bundle weakens 2F5 binding (33).

Discussion

Our results indicate that 2F5 and 4E10 inhibit HIV-1 infection by binding to their epitopes as displayed on the prehairpin intermediate conformation of gp41, thereby blocking a crucial step in the conformational transition required for membrane fusion. Binding may not obstruct formation of the six-helix bundle, however, because the epitopes lie outside HR2; that is, the block may occur at a very late step in the "zipping up" of gp41. These two antibodies could, for example, prevent MPER from interacting with residues proximal to the fusion peptide, a potentially required step for induction of membrane hemifusion. The nonneutralizing, cluster I antibodies bind gp41-inter and prefusion

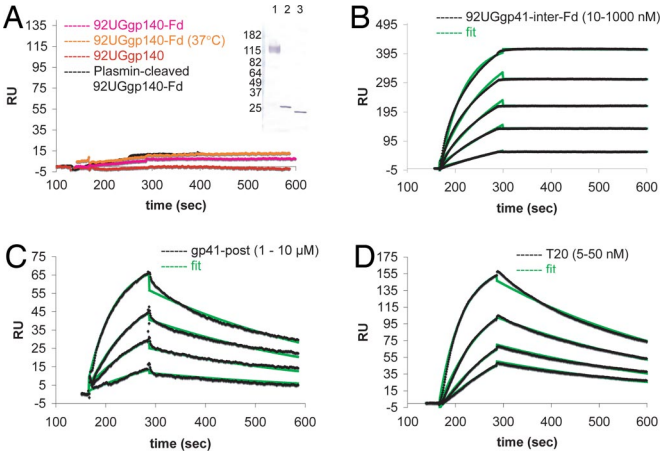

Fig. 3. mAb 2F5 binds the gp41 prehairpin intermediate. (*A*) 2F5 Fab was immobilized on a CM-5 chip, and 92UG-gp140-Fd (1 μM) or 92UG-gp140 (without foldon tag, 1 μM) was the analyte. The sensorgram for 92UG-gp140-Fd is shown in pink, 92UG-gp140-Fd at 37°C in orange, and 92UG-gp140 in red. Plasmin-cleaved 92UG-gp140-Fd was purified by gel-filtration chromatography on a preparation-grade Superdex 200 column; the fraction containing cleaved, trimeric gp140-Fd was immobilized on a Ni-NTA chip (see *SI Methods*); 2F5 Fab at 1 μM was the analyte; the sensorgram is shown in black. mAb 2F5 does not bind to any of the gp140 proteins. (*Inset*) 2F5 does react on an immunoblot with 92UG-gp140-Fd (lane 1), with the two gp41 proteins in the prehairpin intermediate conformation, 92UG-gp41-inter-Fd (lane 2), and HXB2-gp41-inter-GCN4 (lane 3). (*B*) The Fab fragment of 2F5 was immobilized on a CM-5 chip. Solutions at various concentrations of 92UG-gp41-inter-Fd, the gp41-inter protein derived from the 92UG037.8 sequence with a foldon tag, were the analyte. Binding kinetics were evaluated with a 1:1 Langmuir model using BiaEvaluation software (Biacore). The recorded sensorgrams are shown in black and the fits in green. (*C*) The Fab fragment of 2F5 was immobilized on a CM-5 chip. Solutions of 92UG-gp41-post at various concentrations (1.0, 2.5, 5.0, and 10.0 μM) were the analyte. The recorded sensorgrams are in black for 92UG-gp41-post and in green for the fits. (*D*) T20 peptide at different concentrations (5, 10, 25, and 50 nM) was the analyte with a chip bearing immobilized 2F5 Fab. The recorded sensorgrams are in black and the fits in green. Injections were carried out in duplicate and gave essentially the same results. Only one of the duplicates is shown.

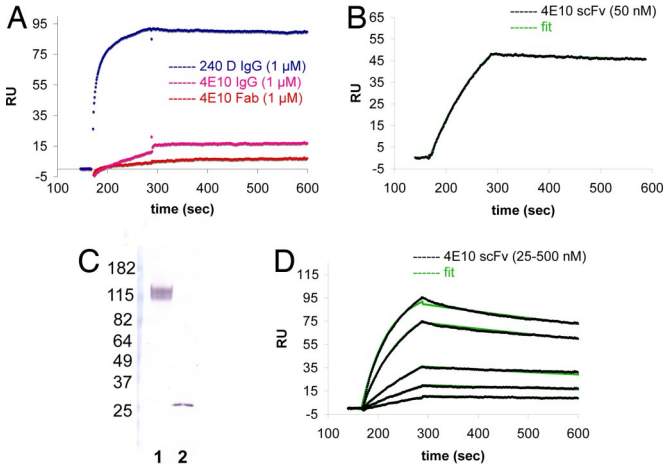

Fig. 4. mAb 4E10 binds the gp41 prehairpin intermediate. (*A*) 92UG-gp140-Fd trimer was immobilized on a Ni-NTA chip, and 4E10 IgG, 4E10 Fab, and 240-D IgG, all at 1 μM, were passed over the surface sequentially. Regeneration was not necessary after binding by 4E10 IgG and Fab. The recorded sensorgrams are in blue for 240-D, in pink for 4E10 IgG, and in red for 4E10 Fab. The 4E10 IgG binds only weakly, even with a potential avidity effect. (*B*) 92UG-gp41-inter was immobilized on a CM-5 chip. 4E10 scFv (50 nM) was the analyte. A duplicate run with the same chip gave lower binding because of the harsh regeneration conditions, but when repeated with a different chip, the results duplicated those shown here. The recorded sensorgrams are in black for 4E10 scFv and in green for the fit. (*C*) Western blot of 92UG-gp140-Fd trimer and 92UG-gp41-inter detected by mAb 4E10. Both 92UG-gp140-Fd (lane 1) and 92UG-gp41-inter (lane 2) react with 4E10. (*D*) Solutions of 4E10 scFv at various concentrations (25–500 nM) were passed over the surface of a SA chip bearing immobilized biotinylated 4E10 epitope peptide. The recorded sensorgrams are in black and the fits in green. All injections were carried out in duplicate and gave essentially the same results (except as described in *B*). Only one of the duplicates is shown in the figure.

gp140 (SI Fig. 6*G* and 7*C*). Thus, binding to the intermediate conformation is not by itself sufficient for neutralization. Because their target is a transient intermediate, 2F5 and 4E10 have a relatively narrow "window of opportunity." Both antibodies, which recognize linear epitopes adjacent to each other in the MPER of gp41, have long, hydrophobic heavy-chain CDR3 loops. These loops contact bound MPER peptides only at their base, and it has been proposed that they also interact with the viral membrane (4, 5). The putative, relatively nonspecific membrane binding may simply concentrate the antibody, to give it a kinetic head start during the short lifetime of the intermediate. Indeed, both 2F5 and 4E10 Fab fragments bind gp41-inter with high affinity in the absence of a lipid bilayer, consistent with a largely kinetic role for any membrane interaction.

Haynes *et al*. (27) have found that 2F5 and 4E10 have properties resembling those of autoreactive antibodies (including their long, heavy-chain CDR3 loops) and that they interact with phospholipids. They suggest that these characteristics might lead to elimination of such heavy chains from the available repertoire. Our data provide an additional explanation for the rarity of 2F5-like antibodies in HIV-infected individuals. The estimated exposure time for a T-20 target site during cell–cell fusion is ≈15 min (34), and the lifetime of an intermediate sensitive to the construct known as "5-helix" may be much lower, only 5–10 s (35). These transient conformations would not have long enough lifetimes to induce a host response effectively. Moreover, they would be present only at the interface of an infecting virion with a T cell or macrophage, inaccessible to the B cell receptor that must initiate clonal proliferation and antibody synthesis.

Various examples from other viruses illustrate that the relevant conformation of a viral envelope protein must be presented, if immunogen design is the goal. The exposure of flavivirus neutralizing epitopes depends on whether the E protein is in a pre- or postfusion conformation (36); a similar conclusion follows from the mapping of antigenic sites on the surfaces of pre- and postfusion vesicular stomatitis virus glycoprotein G (37) and from early studies on antigenicity of influenza virus (38). HIV-1 Env-based protein immunogens often induce high ELISA-titer antibody responses with limited neutralizing activity and breadth (39), but the lack of rigorously characterized preparations of the envelope proteins in well defined conformational states has confused many analyses of antigenicity and immunogenicity. Preparations of recombinant gp140 are often mixtures of monomers and higher oligomers; their conformation and physiological relevance are hard to define. Even cell-associated or virion-associated envelope proteins are structurally heterogeneous because of the tendency for gp120 to dissociate and because of inefficient cleavage of the precursor. The preparations described maybe a useful standard against which to evaluate future immunogens. The tight binding of 2F5 to gp41-inter provides evidence for the significance of an extended, prehairpin intermediate in the fusion transition. Moreover, gp41-inter may provide a scaffold for presenting the MPER in a conformation relevant to neutralization and potentially for inducing a relevant B cell response.

Materials and Methods

Expression Constructs. Expression constructs were generated by standard PCR techniques, as described in detail in *SI Methods*. We used pET21-a(+) (Novagen) to express 92UG-gp41-inter in *E. coli* and pET23-a(+) for HXB2-gp41-inter and

92UG-gp41-post. We used pFastBac-1 (Invitrogen) to express gp140 and gp140-Fd constructs in insect cells. The gp140 contained residues 26–675 (92UG037.8 numbering).

Expression in *E. coli* and Protein Refolding. We expressed gp41-inter and gp41-post in Rosetta (DE3)pLysS cells (Novagen). Cultures were induced at an A_{600} of 1.0 by the addition of 1 mM IPTG. Cells were harvested 2–3 h after induction by centrifugation. Env constructs were insoluble when expressed in *E. coli*. Cells were lysed by three cycles of freezing–thawing in PBS with 0.4 mg/ml DNase I, 0.4 mg/ml RNase A, and 2 mg/ml lysozyme, followed by brief sonication. For His-tagged constructs, inclusion bodies were spun down by centrifugation and solubilized in 6 M guanidine hydrochloride (GnHCl). After removing insoluble material, the supernatant was loaded onto a Ni-NTA resin, washed with 6 M GnHCl, eluted with 300 mM imidazole in 6 M GnHCl. The fractions containing His-tagged protein were pooled, and protein refolding was initiated by rapid dilution into ice-cold refolding buffer [1 M arginine, 100 mM Tris·HCl (pH 7.5), 2 mM EDTA, 0.2 mM oxidized glutathione, 2 mM reduced glutathione, and one protease inhibitor cocktail tablet (Roche)] at a final protein concentration of 100 μg/ml. The refolding mix was stored at 4°C for at least 24 h and then dialyzed against PBS four times and purified on Ni-NTA under native conditions. The imidazole-eluted fractions were pooled, concentrated, and further separated from aggregated species by gel-filtration chromatography on Superdex 200 (GE Healthcare) in 25 mM Tris·HCl (pH 7.5), 150 mM NaCl. Purified protein was concentrated and stored at −80°C. Non-His-tagged gp41 constructs were purified by acid extraction (40). Refolding proceeded as described above, except that the protein was concentrated after dialysis by ultrafiltration with Centricon Plus-70 (Millipore).

SPR. Unless otherwise specified, all experiments were performed in duplicate with a Biacore 3000 instrument (Biacore, Inc.) at 20°C in HBS-EP running buffer [10 mM Hepes (pH 7.4), 150 mM NaCl, 3 mM EDTA, 0.005% surfactant P20]. Immobilization of ligands to CM5, NTA, and SA chips (Biacore) followed the standard procedures recommended by manufacturer. Immobilization of 4E10 antibody to the CM5 chip by the standard amine coupling procedure blocked binding to its antigens; the same protocol also denatured the 92UG-gp140-Fd trimer. These two types of immobilization were therefore not used in the subsequent experiments. The final immobilization levels were between 300 and 500 RU to avoid rebinding events. For kinetic measurements, sensorgrams were obtained by passing various concentrations of an analyte over the ligand surface at a flow rate of 50 μl/min, with a 2-min association phase and a 10-min dissociation phase. The sensor surface was regenerated between each experiment with a single injection of 35 mM NaOH and 1.3 M NaCl, or 10 mM HCl and 1.3 M NaCl, at a flow rate of 100 μl/min. Identical injections over blank surfaces were subtracted from the data for kinetic analysis. Binding kinetics were evaluated with BiaEvaluation software (Biacore).

ACKNOWLEDGMENTS. We thank Stephen Harrison for discussion and critical reading; Zhonghui Ou and Hui Yang for technical assistance; Beatrice Hahn (University of Alabama at Birmingham, Birmingham, AL), Feng Gao, Munir Alam, and Barton Haynes (Duke University, Durham, NC), Hermann Katinger (Institute for Applied Microbiology, University of Agriculture, Vienna), James Robinson (Tulane University, New Orleans), Susan Zolla-Pazner (New York University, New York), Dennis Burton and Ian Wilson (The Scripps Research Institute, La Jolla, CA), and National Institutes of Health AIDS research and reference reagent program for reagents; John Skehel, Barton Haynes, Munir Alam, and Dan Barouch, for comments. The work was supported by grants from National Institutes of Health and the Bill and Melinda Gates Foundation.

1. Wei X, *et al.* (2003) Antibody neutralization and escape by HIV-1. *Nature* 422:307–312.
2. Burton DR, *et al.* (1994) Efficient neutralization of primary isolates of HIV-1 by a recombinant human monoclonal antibody. *Science* 266:1024–1027.
3. Trkola A, *et al.* (1996) Human monoclonal antibody 2G12 defines a distinctive neutralization epitope on the gp120 glycoprotein of human immunodeficiency virus type 1. *J Virol* 70:1100–1108.
4. Cardoso RM, *et al.* (2005) Broadly neutralizing anti-HIV antibody 4E10 recognizes a helical conformation of a highly conserved fusion-associated motif in gp41. *Immunity* 22:163–173.
5. Ofek G, *et al.* (2004) Structure and mechanistic analysis of the anti-human immunodeficiency virus type 1 antibody 2F5 in complex with its gp41 epitope. *J Virol* 78:10724–10737.
6. Harrison SC (2005) Mechanism of membrane fusion by viral envelope proteins. *Adv Virus Res* 64:231–259.
7. Chan DC, Kim PS (1998) HIV entry and its inhibition. *Cell* 93:681–684.
8. Kilby JM, Eron JJ (2003) Novel therapies based on mechanisms of HIV-1 cell entry. *N Engl J Med* 348:2228–2238.
9. Eckert DM, Malashkevich VN, Hong LH, Carr PA, Kim PS (1999) Inhibiting HIV-1 entry: Discovery of D-peptide inhibitors that target the gp41 coiled-coil pocket. *Cell* 99:103–115.
10. Skehel JJ, Wiley DC (2000) Receptor binding and membrane fusion in virus entry: The influenza haemagglutinin. *Annu Rev Biochem* 69:531–569.
11. Jeffs SA, *et al.* (2004) Expression and characterisation of recombinant oligomeric envelope glycoproteins derived from primary isolates of HIV-1. *Vaccine* 22:1032–1046.
12. Yang X, *et al.* (2002) Highly stable trimers formed by human immunodeficiency virus type 1 envelope glycoproteins fused with the trimeric motif of T4 bacteriophage fibritin. *J Virol* 76:4634–4642.
13. Chen B, *et al.* (2000) Expression, purification, and characterization of gp160e, the soluble, trimeric ectodomain of the simian immunodeficiency virus envelope glycoprotein, gp160. *J Biol Chem* 275:34946–34953.
14. Chen B, *et al.* (2004) A chimeric protein of simian immunodeficiency virus envelope glycoprotein gp140 and *Escherichia coli* aspartate transcarbamoylase. *J Virol* 78:4508–4516.
15. Rits-Volloch S, Frey G, Harrison SC, Chen B (2006) Restraining the conformation of HIV-1 gp120 by removing a flexible loop. *EMBO J* 25:5026–5035.
16. Binley JM, *et al.* (2004) Comprehensive cross-clade neutralization analysis of a panel of anti-human immunodeficiency virus type 1 monoclonal antibodies. *J Virol* 78:13232–13252.
17. Zhou T, *et al.* (2007) Structural definition of a conserved neutralization epitope on HIV-1 gp120. *Nature* 445:732–737.
18. Thali M, *et al.* (1993) Characterization of conserved human immunodeficiency virus type 1 gp120 neutralization epitopes exposed upon gp120-CD4 binding. *J Virol* 67:3978–3988.
19. Xu JY, Gorny MK, Palker T, Karwowska S, Zolla-Pazner S (1991) Epitope mapping of two immunodominant domains of gp41, the transmembrane protein of human immunodeficiency virus type 1, using 10 human monoclonal antibodies. *J Virol* 65:4832–4838.
20. Kim M, *et al.* (2001) The stoichiometry of trimeric SIV glycoprotein interaction with CD4 differs from that of anti-envelope antibody Fab fragments. *J Biol Chem* 276:42667–42676.
21. Nyambi PN, *et al.* (2000) Conserved and exposed epitopes on intact, native, primary human immunodeficiency virus type 1 virions of group M. *J Virol* 74:7096–7107.
22. Schulke N, *et al.* (2002) Oligomeric and conformational properties of a proteolytically mature, disulfide-stabilized human immunodeficiency virus type 1 gp140 envelope glycoprotein. *J Virol* 76:7760–7776.
23. Cavacini LA, Duval M, Robinson J, Posner MR (2002) Interactions of human antibodies, epitope exposure, antibody binding and neutralization of primary isolate HIV-1 virions. *AIDS* 16:2409–2417.
24. Hart ML, Saifuddin M, Spear GT (2003) Glycosylation inhibitors and neuraminidase enhance human immunodeficiency virus type 1 binding and neutralization by mannose-binding lectin. *J Gen Virol* 84:353–360.
25. Finnegan CM, Berg W, Lewis GK, DeVico AL (2002) Antigenic properties of the human immunodeficiency virus transmembrane glycoprotein during cell–cell fusion. *J Virol* 76:12123–12134.
26. Sattentau QJ, Zolla-Pazner S, Poignard P (1995) Epitope exposure on functional, oligomeric HIV-1 gp41 molecules. *Virology* 206:713–717.
27. Haynes BF, *et al.* (2005) Cardiolipin polyspecific autoreactivity in two broadly neutralizing HIV-1 antibodies. *Science* 308:1906–1908.
28. de Rosny E, Vassell R, Jiang S, Kunert R, Weiss CD (2004) *J Virol* 78:2627–2631.
29. Binley JM, *et al.* (2003) Binding of the 2F5 monoclonal antibody to native and fusion-intermediate forms of human immunodeficiency virus type 1 gp41: Implications for fusion-inducing conformational changes. *J Virol* 77:5678–5684.
30. Dimitrov AS, *et al.* (2007) Exposure of the membrane-proximal external region of HIV-1 gp41 in the course of HIV-1 envelope glycoprotein-mediated fusion. *Biochemistry* 46:1398–1401.
31. Follis KE, Larson SJ, Lu M, Nunberg JH (2002) Genetic evidence that interhelical packing interactions in the gp41 core are critical for transition of the human immunodeficiency virus type 1 envelope glycoprotein to the fusion-active state. *J Virol* 76:7356–7362.
32. Ho J, *et al.* (2005) Conformational constraints imposed on a pan-neutralizing HIV-1 antibody epitope result in increased antigenicity but not neutralizing response. *Vaccine* 23:1559–1573.
33. Gorny MK, Zolla-Pazner S (2000) Recognition by human monoclonal antibodies of free and complexed peptides representing the prefusogenic and fusogenic forms of human immunodeficiency virus type 1 gp41. *J Virol* 74:6186–6192.
34. Muñoz-Barroso I, Durell S, Sakaguchi K, Appella E, Blumenthal R (1998) Dilation of the human immunodeficiency virus-1 envelope glycoprotein fusion pore revealed by the inhibitory action of a synthetic peptide from gp41. *J Cell Biol* 140:315–323.
35. Steger HK, Root MJ (2006) Kinetic dependence to HIV-1 entry inhibition. *J Biol Chem* 281:25813–25821.
36. Modis Y, Ogata S, Clements D, Harrison SC (2004) Structure of the dengue virus envelope protein after membrane fusion. *Nature* 427:313–319.
37. Roche S, Rey FA, Gaudin Y, Bressanelli S (2007) Structure of the prefusion form of the vesicular stomatitis virus glycoprotein G. *Science* 315:843–848.
38. Daniels RS, Douglas AR, Skehel JJ, Wiley DC (1983) Analyses of the antigenicity of influenza haemagglutinin at the pH optimum for virus-mediated membrane fusion. *J Gen Virol* 64:1657–1662.
39. Bower JF, Li Y, Wyatt R, Ross TM (2006) HIV-1 Envgp140 trimers elicit neutralizing antibodies without efficient induction of conformational antibodies. *Vaccine* 24:5442–5451.
40. Frey G, *et al.* (2006) Small molecules that bind the inner core of gp41 and inhibit HIV envelope-mediated fusion. *Proc Natl Acad Sci USA* 103:13938–13943.